CESR LATTICE FOR TWO BEAM OPERATIONS WITH NARROW GAP UNDULATORS AT CHESS*

S.T. Wang#, D. L. Rubin, J. Shanks, CLASSE, Cornell University, Ithaca, NY 14853, USA

Abstract

CESR has operated as a dedicated light source since the conclusion of colliding beam program in 2008. Two undulators with a 6.5mm-vertical gap were installed in Fall 2014, replacing a wiggler in the sextant of CESR that is the home to all CHESS beam lines. In order to operate narrow gap undulators with two beams, CESR pretzel lattice was redesigned so that e^- and e^+ orbits are coincident in one machine sextant but separated in return arcs. In particular both e^- and e^+ orbits are on axis through undulators. This "arc-pretzel" lattice has been the basis for undulator operation. To better understand the beam dynamics and improve machine performance, we developed many simulation tools: undulator modelling, injection tracking, etc. With installation of an additional quadrupole near undulators, the CESR lattice is further modified with a low beta waist in the insertion devices, allowing a more than two fold reduction of local beta functions. This reduction is anticipated to mitigate the effects of small aperture and undulator field errors and to enhance the x-ray brightness. The characterization of the lattice are compared with measurements of injection efficiency, tune scans, etc.

INTRODUCTION

The Cornell Electron Storage Ring (CESR) was built underground on the Cornell University campus in 1979 with a circumference of ~768 m. It stores counter-rotating beams of electrons and positrons that are accelerated to high energy by the Cornell Synchrotron. Figure 1 shows the schematic layout of Linac, Synchrotron, and CESR. Positrons circulate in the clock-wise direction in CESR and electrons in the counter clock-wise direction. Using pretzel orbits generated by electrostatic separators, CESR operated as an electron-positron collider for nearly three decades. Because ring energy can be easily configured in the range of 1.5 to 5.3 GeV, CESR has also been used as a test accelerator (CESR-TA) for exploring the physics and technologies of low emittance rings since 2008 [1].

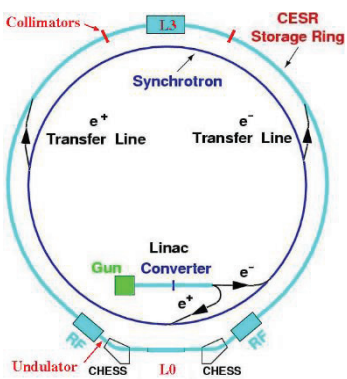

Figure 1: CESR layout and undulator location.

Since the conclusion of colliding beam program, CESR is primarily used as a dedicated x-ray source for a state-of-the-art x-ray facility, known as the Cornell High Energy Synchrotron Source (CHESS). CHESS was built to take advantage of the two-beam running conditions. Therefore, half of beam lines utilize synchrotron radiation from the positron beam and half from the electron beam, as indicated in Fig. 1. The orbits of the electron and positron beams for CHESS operation prior to the installation of undulators are shown in Fig. 2(a). Note that the closed orbits are never coincident. To increase x-ray flux, two undulators with a 6.5mm-vertical gap (chamber gap 4.5mm) were built [2] and installed in Fall 2014, replacing a wiggler which provided beam for five beam lines (Fig. 1). The compact undulators have a very narrow good field region: the vertical field (B_y) rolls off ~10% within x=±9mm. However, as shown in Fig. 2(a), both e^- and e^+ orbits have large horizontal displacement ~15 mm at the undulators. Indeed the pretzel configuration with differential closed orbit that extends around the ring is incompatible with the compact undulator.

In order to operate narrow gap undulators with two beams, CESR pretzel lattice was redesigned so that e^- and e^+ orbits are coincident in one machine sextant but separated in the return arcs. In particular both e^- and e^+ orbits are on axis through the undulators. The orbits of the new lattice are shown in Fig. 2(b). The s=0 location is at the centre of CHESS user region. The green lines in Fig. 2(b) indicate the undulator locations, at which both beams have less than 0.3 mm displacement from the centre. This "arc-pretzel" lattice has been the basis for all two beam undulator operation.

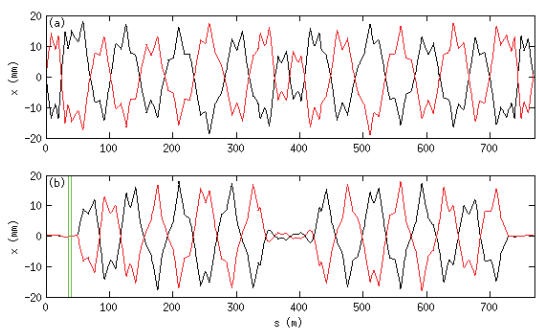

Figure 2: The e^+ (black) and e^- (red) pretzel orbit used (a) before and (b) after undulator installation.

OPERATION

Lattice parameters of recent arc pretzel lattice named "Arc pretz" are listed in Table 1. Compared to the pre-

*Work supported by NSF DMR-0936384 and NSF DMR-1332208
#sw565@cornell.edu

undulator lattice "Old pretz", its emittance reduced by one third as a result of the increased horizontal tune. Twiss parameters at several locations of around the storage ring have also been optimized to minimize the particle loss at the undulators during injection. First, β_y at centre of the undulators is decreased by half (Table 1). Secondly, β_x at the injection points was increased to 50 m to reduce the horizontal oscillation amplitude elsewhere in the ring and improve injection efficiency. Thirdly, two vertical collimators with vertical gaps of 7 and 10 mm respectively were installed in the north arc (Fig. 1). The nominal vertical aperture is 45 mm. Vertical beta (β_y) at these locations is increased to 50 m. In addition, the phase advance between one of collimators and the undulator was optimized to be half integer or integer. This arrangement ensures that injected particles with large vertical oscillation amplitude will be blocked by the collimators rather than striking the undulators.

Machine operation with undulators in the arc pretzel lattice was initially very challenging. With the undulators in place machine conditions were fragile; in particular, it was difficult to maintain injection efficiency, which at high current became increasingly sensitive to the betatron tunes. Experimental tune scans showed the region in the tune plane with good lifetime shrank after installing undulators. To better understand the beam dynamics and improve machine performance, we developed simulation tools: improved undulator modelling, injection tracking, etc. which will be discussed in the following sections.

Table 1: Lattice Parameters

Lattice	ε_x (nm)	Q_x	Q_y	β_x (m)	β_y (m)
Old pretz	145	10.541	9.602	22.6	11.3
Arc pretz	103	11.276	8.784	28.1	6.8
Low beta	99	11.282	8.784	7.7	3.2

UNDULATOR MODEL

The 1.5-m long undulators installed in CESR are designed by Cornell and manufactured by KYMA S.r.l [2]. Each undulator consists of 104 poles made of permanent magnets. Fig. 3(a) shows the horizontal $B_y(x)$ profile in the middle plane and z=0 positions calculated with the Opera software [3]. The peak field $B_y(0)$ is about 0.93 T.

The undulator was modelled in two steps in BMAD, which is a subroutine library for relativistic charged-particle dynamics simulations [4]. The first step is to build a field model B(x, y, z) with a similar approach to that described in [5]. $B_y(x, 0, 0)$ was fitted with a 27-term cosine expansion as shown in Fig. 3(a). Since the undulator has planar symmetry and the field along s is periodic, B_x, B_y, and B_z, are constructed with 27 B_n terms [4, 5]. Because of non-uniformities in the field, the undulator has intrinsic dynamic field integrals (green line in Fig. 3a). Due to assembly or alignment errors, there will be additional finite errors in the actual field map. These field errors are quantified by static field integrals [6]. Fig. 3(b) and (c) show measured undulator field integrals $I_y(x, y=0)$ and $I_x(x, y=0)$, respectively. These field integrals also give the particle finite transverse kicks when it passes through the undulator [6]. Our second step is to model the static field integrals. Using the same strategy as constructing the undulator field model, we first fit $I_x(x, y=0)$ and $I_y(x, y=0)$ with cosine terms and then construct $I_x(x, y)$ and $I_y(x, y)$ based on these cosine terms [4]. The kicks due to the field integrals are then applied to the particle within a custom tracking code using a symplectic tracking routine.

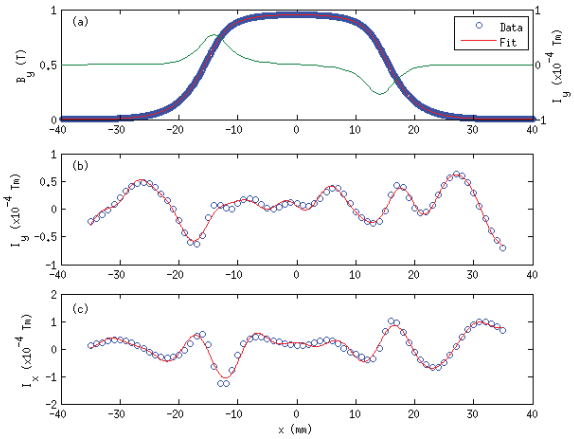

Figure 3: B_y, measured field integral I_x and I_y of KYMA undulator. Symbols are the data and red line is the fit.

MULTIPOLES AND BBI

Besides the undulator model, nonlinear field components from CESR elements such as dipoles, quadrupoles, sextupoles, vertical steerings in sextupole magnets, and horizontal electrostatic separators, have been included in the lattice model [7]. In BMAD, the effective nonlinearity of an element is included as multipoles to the element structure. The strength of these multipoles are proportional to the main element strength. For example, the quadrupole multipoles scale with the strength of the quadrupole. The multipoles associated with vertical steerings similarly scale with the actual deflection angles calculated based on machine running conditions [8].

Another important effect that is incorporated in the tracking model is the long range beam-beam interaction (BBI) at the parasitic crossing points of the multiple bunches in the two beams [9]. BBI is computed in a weak-strong approximation, where beam functions of one beam (strong) are held fixed and the effect on the weak other beam is calculated for the individual macro-particles. Special BBI elements are inserted in the ring lattice at those parasitic crossing locations. When the weak beam tracks through those elements, a beam-beam kick will be applied based on the beam size, and particle numbers of the strong beam. The beam-beam kick is computed using the Bassetti–Erskine complex error function formula [10].

ISBN 978-3-95450-147-2

SIMULATION

As noted above, with installation of undulators, the primary operational impact was with respect to injection. Our model of the injection process attempts to include all of the relevant physics. In addition to the undulator model, magnet multipoles, and BBI mentioned above, the sextupoles in the tracking model are tuned to the measured chromaticity and tonality (tune split of the opposing beams). The apertures of ring vacuum chambers, collimators, etc. are also included in the tracking lattice.

The injection simulation is based on work in a previous report [11]. 200 injected particles are launched at the injection point and tracked through the lattice for 400 turns. If the particle survives for 400 turns, it is flagged as captured. The injection efficiency is the percentage of injected particles that survived for 400 turns. The initial 6D orbit coordinates of 200 particles are generated randomly based on the measured emittance of the injected beam at the end of transfer line. The horizontal centre of 200 particles is displaced 17 mm from the closed orbit of stored beam to reflect the measured initial injection oscillation amplitude. The Twiss parameters of the injected beam at the end of transfer line are matched to into the storage ring.

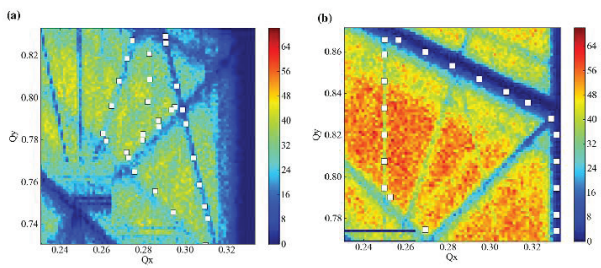

Figure 4: Positron injection tune scan for (a) "Arc pretz" lattice and (b) "Low beta" lattice.

Figure 4(a) shows a positron injection tune scan from "Arc pretz" lattice with realistic 4 ns electron bunch pattern and 4 mA per bunch current. The colour scale indicates injection efficiency. The white squares on the plot are the experimentally-measured tune plane boundary, within which the lifetime of the stored positron beam is good. It was measured by checking positron life time while scanning tunes with injection pulsed bump turned on. The measured resonant lines are consistent with resonances that appear in the simulation. The good operating region is small. In addition, many higher order resonant lines are present. Overall, the injection efficiency is much less than 50%, consistent with actual machine injection conditions in CESR. Further simulation with lattice including only undulator field roll-off or field integral model indicates that field integrals from the undulator are likely responsible for the poor injection efficiency.

Figure 3 indicates that both dynamic and static field integrals are much smaller when the trajectories are nearer the centre of undulator (x=±10mm). Therefore, the

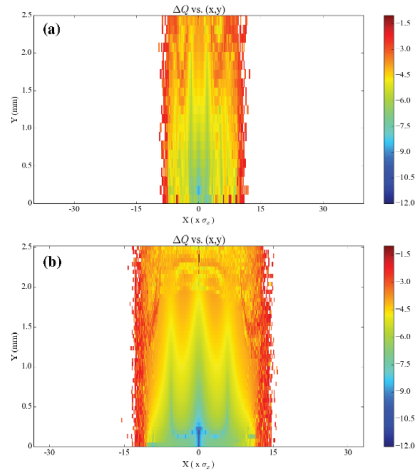

Figure 5: Dynamic aperture of (a) "Arc pretz" and (b) "Low beta" lattice.

deleterious effect of field integrals is reduced by minimizing both horizontal and vertical beta at the undulators. An additional quadrupole was added near the undulators to generate a low beta waist in the insertion devices. Table 1 shows that more than two fold reduction of local beta functions is achieved.

Injection simulations as well as frequency map analysis [12] were performed to check beam dynamics of the "Low beta" lattice. Figure 4(b) shows that injection efficiency is dramatically improved (>50% efficiency). The width of a few higher order resonant lines was reduced. Others disappeared entirely. The frequency analysis in Fig. 5 also indicates dynamic aperture of "Low beta" lattice is significantly greater than for the "Arc pretz" lattice with $\pm 15\sigma_x$ horizontal aperture. The vertical aperture is limited by the physical aperture of undulator chamber. Since February 2016, CHESS started operation with the low beta lattice, and we observed improved positron injection efficiency >60%. In addition, the measured good lifetime tune region is significantly expanded as shown in Fig. 4(b). These observations are consistent with our simulation results.

CONCLUSION

Simulation tools such as undulator modelling, injection tune scan, and frequency map analysis were developed to investigate several arc pretzel lattices for CHESS undulator operation. The simulation results are consistent with experimental observations in machine tuning. It provided guidance for installation of an additional quad to generate a low beta waist in the insertion devices, which improved operation conditions dramatically.

ACKNOWLEDGMENT

We thank CESR operation group for machine study support.

REFERENCES

[1] M.A. Palmer et al., "The Conversion and Operation of the Cornell Electron Storage Ring as a Test Accelerator (CesrTA) for Damping Rings Research and Development," PAC'09, Vancouver, June 2009, p. 4200 (2009).

[2] A. Temnykh et al., "Construction of CHESS compact undulator magnets at Kyma," Proc. of SPIE Vol. 9512 951205-6 (2015).

[3] http://operafea.com/

[4] D. Sagan, The BMAD Reference Manual, http://www.lepp.cornell.edu/~dcs/bmad/

[5] D. Sagan et al., "A magnet field model for wigglers and undulators," PAC'03, Portland, May 2013, p. 1023 (2013).

[6] Z. Wolf, "Undulator field integral measurements," LCLS- TN-05-22, July, 2005.

[7] A. Temnykh, "On nonlinear field components of CESR elements," CBN 96-19, Cornell, 1996.

[8] A. Temnykh, "The single beam dynamics study at CESR," CNB 97-2, Cornell, 1997.

[9] D. Rubin, "Optical effects of parasitic crossings with nine trains of bunches," CBN 96-2, Cornell, 1996.

[10] R. Talman, "Physics of Particle Accelerators," AIP Conf. Proc. No. 153, p. 789, (1997).

[11] D. Rice et al., "Injection measurements in CESR," CNB 92-8, Cornell, 1992.

[12] L. Nadolski et al., "Review of single particle dynamics for third generation light sources through frequency map analysis," PRSTAB, 6, p 114801 (2003).

ISBN 978-3-95450-147-2